

## Lifetime of metastable states and suppression of noise in Interdisciplinary Physical Models \*

B. SPAGNOLO<sup>a†</sup>, A. A. DUBKOV<sup>b</sup>, A. L. PANKRATOV<sup>c</sup>,  
E. V. PANKRATOVA<sup>d</sup>, A. FIASCONARO<sup>a,e,f</sup>, A. OCHAB-MARCINEK<sup>e</sup>

<sup>a</sup>Dipartimento di Fisica e Tecnologie Relative, Università di Palermo  
CNISM - Unità di Palermo, Group of Interdisciplinary Physics<sup>‡</sup>  
Viale delle Scienze, I-90128 Palermo, Italy

<sup>b</sup>Radiophysics Department, Nizhny Novgorod State University, 23 Gagarin ave.,  
603950 Nizhny Novgorod, Russia

<sup>c</sup>Institute for Physics of Microstructures of RAS, GSP-105, Nizhny Novgorod,  
603950, Russia

<sup>d</sup>Mathematical Department, Volga State Academy, Nesterov street 5,  
Nizhny Novgorod, 603600, Russia

<sup>e</sup>Marian Smoluchowski Institute of Physics, Jagellonian University  
Reymonta 4, 30059 Krakw, Poland

<sup>f</sup>Mark Kac Center for Complex Systems Research, Jagellonian University  
Reymonta 4, 30059 Krakw, Poland

Transient properties of different physical systems with metastable states perturbed by external white noise have been investigated. Two noise-induced phenomena, namely the noise enhanced stability and the resonant activation, are theoretically predicted in a piece-wise linear fluctuating potential with a metastable state. The enhancement of the lifetime of metastable states due to the noise, and the suppression of noise through resonant activation phenomenon will be reviewed in models of interdisciplinary physics: (i) dynamics of an overdamped Josephson junction; (ii) transient regime of the noisy FitzHugh-Nagumo model; (iii) population dynamics.

PACS numbers: 05.10.-a, 05.40.-a, 87.23.Cc

---

\* Presented at the 19<sup>th</sup> Marian Smoluchowski Symposium on Statistical Physics, Kraków, Poland, May 14-17, 2006

† e-mail: spagnolo@unipa.it

‡ <http://gip.dft.unipa.it>

## 1. Introduction

Metastability is a generic feature of many nonlinear systems, and the problem of the lifetime of metastable states involves fundamental aspects of nonequilibrium statistical mechanics. Nonequilibrium systems are usually open systems which strongly interact with environment through exchanging materials and energy, which can be modelled as noise. The investigation of noise-induced phenomena in far from equilibrium systems is one of the approaches used to understand the behaviour of physical and biological complex systems. Specifically the relaxation in many natural complex systems proceeds through metastable states and this transient behaviour is observed in condensed matter physics and in different other fields, such as cosmology, chemical kinetics, biology and high energy physics [1]-[9]. In spite of such ubiquity, the microscopic understanding of metastability still raises fundamental questions, such as those related to the fluctuation-dissipation theorem in transient dynamics [10].

Recently, the investigation of the thermal activated escape in systems with fluctuating metastable states has led to the discovery of resonancelike phenomena, characterized by a nonmonotonic behavior of the lifetime of the metastable state as a function of the noise intensity or the driving frequency. Among these we recall two of them, namely the resonant activation (RA) phenomenon [11]-[21], whose signature is a minimum of the lifetime of the metastable state as a function of a driving frequency, and the noise enhanced stability (NES) [3], [17]-[27]. This resonancelike effect, which contradicts the monotonic behavior predicted by the Kramers formula [28, 29], shows that the noise can modify the stability of the system by enhancing the lifetime of the metastable state with respect to the deterministic decay time. Specifically when a Brownian particle is moving in a potential profile with a fluctuating metastable state, the NES effect is always obtained, regardless of the unstable initial position of the particle. Two different dynamical regimes occur. These are characterized by: (i) a monotonic behavior with a divergence of the lifetime of the metastable state when the noise intensity tends to zero, for a given range of unstable initial conditions (see for detail Ref. [24]), which means that the Brownian particle will be trapped into the metastable state in the limit of very small noise intensities; (ii) a nonmonotonic behavior of the lifetime of the metastable state as a function of noise intensity. The noise enhanced stability effect implies that, under the action of additive noise, a system remains in the metastable state for a longer time than in the deterministic case, and the escape time has a maximum as a function of noise intensity. We can lengthen or shorten the mean lifetime of the metastable state of our physical system, by acting on the white noise intensity. The noise-induced stabilization, the noise induced slowing

down in a periodical potential, the noise induced order in one-dimensional map of the Belousov-Zhabotinsky reaction, and the transient properties of a bistable kinetic system driven by two correlated noises, are akin to the NES phenomenon [22].

In this paper we will review these two noise-induced effects in models of interdisciplinary physics, ranging from condensed matter physics to biophysics. Specifically in the first section, after shortly reviewing the theoretical results obtained with a model based on a piece-wise linear fluctuating potential with a metastable state, we focus on the noise-induced effects RA and NES. In the next sections, we show how the enhancement of the lifetime of metastable states due to the noise and the suppression of noise, through resonant activation phenomenon, occur in the following interdisciplinary physics models: (i) dynamics of an overdamped Josephson junction; (ii) transient regime of the noisy FitzHugh-Nagumo model; (iii) population dynamics.

## 2. The model

As an archetypal model for systems with a metastable state and strongly coupled with the noisy environment, we consider the one-dimensional overdamped Brownian motion in a fluctuating potential profile

$$\frac{dx}{dt} = -\frac{\partial [U(x) + V(x)\eta(t)]}{\partial x} + \xi(t), \quad (1)$$

where  $x(t)$  is the displacement of the Brownian particle and  $\xi(t)$  is the white Gaussian noise with the usual statistical properties:  $\langle \xi(t) \rangle = 0$ ,  $\langle \xi(t)\xi(t') \rangle = 2D \delta(t-t')$ . The variable  $\eta(t)$  is the Markovian dichotomous noise, which takes the values  $\pm 1$  with the mean flipping rate  $\nu$ . The potential profile  $U(x) + V(x)$  corresponds to a metastable state, and  $U(x) - V(x)$  corresponds to an unstable one, with a reflecting boundary at  $x \rightarrow -\infty$  and an absorbing boundary at  $x \rightarrow +\infty$  (see Fig. 1). Starting from the well-known expression for the probability density of the process  $x(t)$

$$P(x, t) = \langle \delta(x - x(t)) \rangle \quad (2)$$

and using the auxiliary function  $Q(x, t)$

$$Q(x, t) = \langle \eta(t) \delta(x - x(t)) \rangle, \quad (3)$$

and the Eq. (1), we obtain the set of differential equations

$$\frac{\partial P(x, t)}{\partial t} = \frac{\partial}{\partial x} [U'(x)P + V'(x)Q] + D \frac{\partial^2 P}{\partial x^2},$$

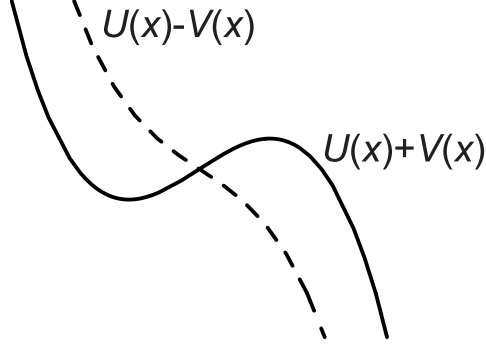


Fig. 1. Switching potential with metastable state.

$$\frac{\partial Q(x, t)}{\partial t} = -2\nu Q + \frac{\partial}{\partial x} [U'(x) Q + V'(x) P] + D \frac{\partial^2 Q}{\partial x^2}. \quad (4)$$

The average lifetime of Brownian particles in the interval  $(L_1, L_2)$ , with the initial conditions  $P(x, 0) = \delta(x - x_0)$  and  $Q(x, 0) = \pm \delta(x - x_0)$ , is

$$\tau(x_0) = \int_0^\infty dt \int_{L_1}^{L_2} P(x, t | x_0, 0) dx = \int_{L_1}^{L_2} Y(x, x_0, 0) dx, \quad (5)$$

where  $Y(x, x_0, s)$  is the Laplace transform of the conditional probability density  $P(x, t | x_0, 0)$ . After Laplace transforming Eqs. (4), with above-mentioned initial conditions and using the method proposed in Refs. [25, 26, 30], we can express the lifetime  $\tau(x_0)$  as

$$\tau(x_0) = \int_{L_1}^{L_2} Z_1(x, x_0) dx, \quad (6)$$

where  $Z_1(x, x_0)$  is the linear coefficient of the expansion of the function  $sY(x, x_0, s)$  in a power series in  $s$ . By Laplace transforming the auxiliary function  $Q(x, t)$  in  $R(x, x_0, s)$ , and expanding the function  $sR(x, x_0, s)$  in similar power series, we obtain the following closed set of integro-differential equations for the functions  $Z_1(x, x_0)$  and  $R_1(x, x_0)$  [17]

$$\begin{aligned} DZ_1' + U'(x) Z_1 + V'(x) R_1 &= -\theta(x - x_0), \\ DR_1' + U' R_1 + V' Z_1 &= 2\nu \int_{-\infty}^x R_1 dy \mp \theta(x - x_0), \end{aligned} \quad (7)$$

where  $\theta(x - x_0)$  is the Heaviside step function, and  $R_1(x, x_0)$  is the linear coefficient of the expansion of the function  $sR(x, x_0, s)$ . We put equal to zero the probability flow at the reflecting boundary  $x = -\infty$ . These general

equations (6) and (7) allow to calculate the average lifetime for potential profiles with metastable states. We may consider two mean lifetimes  $\tau_+(x_0)$  and  $\tau_-(x_0)$ , depending on the initial configuration of the randomly switching potential profile:  $U(x) + V(x)$  or  $U(x) - V(x)$ . The average lifetime (6) is equal to  $\tau_+(x_0)$ , when we take the sign "–" in the second equation of system (7), and vice versa for  $\tau_-(x_0)$ .

We consider now the following piece-wise linear potential profile

$$U(x) = \begin{cases} +\infty, & x < 0 \\ 0, & 0 \leq x \leq L \\ k(L-x), & x > L \end{cases} \quad (8)$$

and  $V(x) = ax$  ( $x > 0$ ,  $0 < a < k$ ). Here we consider the interval  $L_1 = 0$ ,  $L_2 = b$ , with  $b > L$ . After solving the differential equations (7) with the potential profile (8), and by choosing the initial position of Brownian particles at  $x = 0$ , we get the exact mean lifetime

$$\tau_-(x_{in} = 0) = \frac{b}{k} + \frac{\nu L^2}{\Gamma^2} + \frac{a}{2\nu\Gamma^4} f(D, \Gamma, \nu), \quad (9)$$

where  $\Gamma = \sqrt{a^2 + 2\nu D}$ . Here  $f(D, \Gamma, \nu)$ , which is also a function of the potential parameters  $a, b, L, k$ , has a complicated expression in terms of parameters  $D, \Gamma$  and  $\nu$  [17]. It is worthwhile to note that Eq. (9) was derived without any assumptions on the white noise intensity  $D$  and on the mean rate of flippings  $\nu$  of the potential.

To look for the NES effect, which is observable at very small noise intensity [3, 23], we derive the average life time in the limit  $D \rightarrow 0$

$$\tau_-(x_{in} = 0) = \tau_0 + \frac{D}{a^2} g(q, \omega, s) + o(D), \quad (10)$$

where  $\omega = \nu L/k$ ,  $q = a/k$  and  $s = 2\omega(b/L - 1)/(1 - q^2)$  are dimensionless parameters. Here

$$g(q, \omega, s) = \frac{3q^2 + 4q - 5}{2(1 - q^2)} + 2\omega \frac{3q^2 + q - 3}{q(1 - q^2)} - \frac{2\omega^2}{q^2} + se^{-s} \frac{q^3(1 + q^2)}{(1 + q)(1 - q^2)} + (1 - e^{-s}) \frac{q(1 - q^2 - 2q^3)}{2(1 - q^2)} \quad (11)$$

and

$$\tau_0 = \frac{2L}{a} + \frac{\nu L^2}{a^2} + \frac{b - L}{k} - \frac{q(1 - q)}{2\nu} (1 - e^{-s}) \quad (12)$$

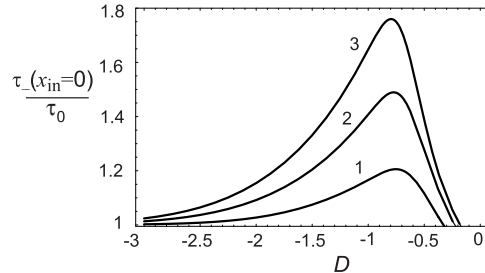


Fig. 2. Semilogarithmic plot of the normalized mean lifetime  $\tau_{-}(x_{in}=0)/\tau_0$  vs the white noise intensity  $D$  for three values of the dimensionless mean flipping rate  $\omega = \nu L/k$ : 0.03 (curve 1), 0.01 (curve 2), 0.005 (curve 3). Parameters are  $L = 1$ ,  $k = 1$ ,  $b = 2$ , and  $a = 0.995$ .

is the mean lifetime in the absence of white Gaussian noise ( $D = 0$ ). The condition to observe the NES effect can be expressed by the inequality

$$g(q, \omega, s) > 0. \quad (13)$$

The main conclusions from the analysis of the inequality (13) are: (i) the NES effect occurs at  $q \simeq 1$ , i.e. at very small steepness  $k - a = k(1 - q)$  of the reverse potential barrier for the metastable state: for this potential profile, a small noise intensity can return particles into potential well, after they crossed the point  $L$ ; (ii) for a fixed mean flipping rate, the NES effect increases when  $q \rightarrow 1$ , and (iii) for fixed parameter  $q$  the effect increases when  $\omega \rightarrow 0$ , because Brownian particles have enough time to move back into potential well.

Under very large noise intensity  $D$ , the Brownian particles "do not see" the fine structure of potential profile and move as in the fixed potential  $U(x) = -kx$ . Therefore the average life time decreases with noise intensity, tending to the value  $b/k$  as follows from Eq. (9) in the limit  $D \rightarrow \infty$ . In Fig. 2 we show the plots of the normalized mean lifetime  $\tau_{-}(x_{in}=0)/\tau_0$ , Eq. (9), as a function of the noise intensity  $D$  for three values of the dimensionless mean flipping rate  $\omega = \nu L/k$ : 0.03, 0.01, 0.005. The values of the parameters of the potential profile are:  $L = k = 1$ ,  $a = 0.995$ ,  $b = 2$ . The maximum value of the average lifetime and the range of noise intensity values, where NES effect occurs, increases when  $\omega$  decreases. By using exact Eq. (9) we have also investigated the behaviour of the mean lifetime  $\tau_{-}(x_{in}=0)$  as a function of switchings mean rate  $\nu$  of the potential profile. In Fig. 3 we plot this behaviour for six values of the noise intensity, namely:  $D = 0.08, 0.1, 0.13, 0.16, 0.2, 0.25$ . At very slow flippings ( $\nu \rightarrow 0$ ) we obtain

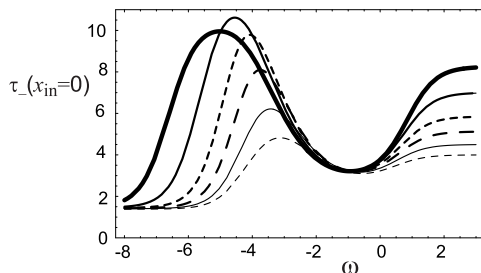


Fig. 3. Semilogarithmic plot of the mean lifetime  $\tau_-(0)$  vs the dimensionless mean flipping rate  $\omega = \nu L/k$  for seven noise intensity values. Specifically from top to bottom on the right side of the figure:  $D = 0.08, 0.1, 0.13, 0.16, 0.2, 0.25$ . The other parameters are the same as in Fig. 2.

$$\tau_{-(\nu \rightarrow 0)}(x_{in} = 0) \simeq \tau_d - \frac{D(1 - e^{-aL/D})}{a^2(1 + q)}, \quad (14)$$

i.e. the average lifetime of the fixed unstable potential  $U(x) - ax$ . Here  $\tau_d = L/a + (b - L)/(k + a)$  is the deterministic time at zero frequency ( $\nu = 0$ ). While for very fast switchings ( $\nu \rightarrow \infty$ ) we obtain

$$\tau_{-(\nu \rightarrow \infty)}(x_{in} = 0) \simeq \frac{b}{k} + \frac{L^2}{2D}, \quad (15)$$

i.e. the mean lifetime for average potential  $U(x)$ . All limiting values of  $\tau_-(x_{in} = 0)$ , expressed by Eqs. (14) and (15), are shown in Fig. 3. At intermediate rates the average escape time from the metastable state exhibits a minimum at  $\omega = 0.1$ , which is the signature of the resonant activation (RA) phenomenon [11]-[15]. If the potential fluctuations are very slow, the average escape time is equal to the average of the crossing times over upper and lower configurations of the barrier, and the slowest process determines the value of the average escape time [11]. In the limit of very fast fluctuations, the Brownian particle "sees" the average barrier and the average escape time is equal to the crossing time over the average barrier. In the intermediate regime, the crossing is strongly correlated with the potential fluctuations and the average escape time exhibits a minimum at a resonant fluctuation rate. Specifically, for  $D \ll 1$  and the parameter values of the potential ( $a = 0.995, L = k = 1, b = 2$ ), we obtain from Eqs. (14) and (15):  $\tau_{-(\nu \rightarrow 0)}(x_{in} = 0) \simeq 1.5 - D/2$ , and  $\tau_{-(\nu \rightarrow \infty)}(x_{in} = 0) \simeq 2 + 1/(2D)$ , that is

$$\tau_{-(\nu \rightarrow 0)}(x_{in} = 0) \ll \tau_{-(\nu \rightarrow \infty)}(x_{in} = 0) \quad (16)$$

which is consistent with the physical picture for which we have at zero frequency of switchings the unstable initial configuration of the potential (see Fig. 1), and at very fast switchings ( $\nu \rightarrow \infty$ ) the average configuration of the potential, which in our case has not barrier. For  $D \gg 1$ , because

$$\lim_{D \rightarrow \infty} D \left(1 - e^{-aL/D}\right) = aL, \quad (17)$$

we have  $\tau_{-(\nu \rightarrow 0)}(x_{in} = 0) = b/(k + a) \simeq 1$ , and  $\tau_{-(\nu \rightarrow \infty)}(x_{in} = 0) = 2$ . So, for the noise intensity values used in our calculations shown in Fig. 3, ranging from  $D = 0.08$  to  $D = 0.25$ , the limiting values for the average lifetime are:  $\tau_{-(\nu \rightarrow 0)}(x_{in} = 0) \simeq (1.38 \div 1.46)$ , and  $\tau_{-(\nu \rightarrow \infty)}(x_{in} = 0) \simeq (4 \div 8)$ , which are consistent with the limiting values shown in Fig. 3, and evaluated directly from exact expression (9).

Moreover, in Fig. 3 a *new resonance-like behaviour*, is observed. The mean lifetime of the metastable state  $\tau_{-}(x_{in} = 0)$  exhibits a *maximum*, between the slow limit of potential fluctuations (static limit) and the RA minimum, as a function of the mean fluctuation rate of the potential, . This maximum occurs for a value of the barrier fluctuation rate on the order of the inverse of the time  $\tau_{up}(D)$  required to escape from the metastable fixed configuration

$$\tau_{up}(D) = \frac{b - L}{k - a} - \frac{L}{a} + \frac{D \left(e^{aL/D} - 1\right)}{a^2(1 - q)}. \quad (18)$$

Specifically we observe that this maximum increases with decreasing noise intensity  $D$  and at the same time the position of the maximum is shifted towards lower values of the dimensionless mean flipping rate  $\omega$ . In fact from Eq. (18) we have that the average time required to escape from the metastable fixed configuration  $\tau_{up}$  increases, consequently the corresponding rate of the barrier fluctuations  $\omega_{max} \simeq 1/\tau_{up}(D)$  decreases, as shown in Fig. 3. We can also estimate the value of the maximum ( $\tau_{-max}(x_{in} = 0)$ ) and its position ( $\omega_{max}$ ), by expanding Eqs. (10)-(12) in a power series up to the second order in  $\omega$ . Using the same parameter values of the potential we have:  $\omega = \nu$ ,  $s = 2\omega/(1 - q^2)$ ,  $se^{-s} \approx s - s^2$ , and  $1 - e^{-s} \approx s - \frac{s^2}{2}$ . We obtain finally:

$$\tau_{-}(x_{in} = 0) \approx 2.5 + (98.7)D + \omega[51 + (347.4)D] - (2 \times 10^6)\omega^2 D. \quad (19)$$

For  $D = 0.1$  we have:  $\tau_{-max} \approx 12.3$  and  $\omega_{max} \approx 2 \times 10^{-4}$ , which are an estimate of the coordinates of the maximum of the corresponding curve in Fig. 3. From small noise intensity  $D \rightarrow 0$ , from Eq. (19), we obtain:  $\tau_{-max} \approx \frac{0.6 \times 10^{-3}}{D} + O(D)$ . The maximum of the average lifetime  $\tau_{-max}$ , therefore, increases when the noise intensity decreases as shown in Fig. 3.



This suggests that, the enhancement of stability of metastable state is strongly correlated with the potential fluctuations, when the Brownian particle "sees" the barrier of the metastable state [3, 17, 23]. When the average time to cross the barrier, that is the average lifetime of the metastable state, is approximately equal to the correlation time of the fluctuations of the potential barrier, a resonance-like phenomenon occurs. In other words, this new effect can be considered as a NES effect in the frequency domain. It is worthwhile to note that the new nonmonotonic behaviour shown in Fig. 3 is in good agreement with experimental results observed in a periodically driven Josephson junction (JJ) [20]. In this very recent paper the authors experimentally observe the coexistence of RA and NES phenomena. Specifically they found (see Fig.3 of the paper [20]) that the maximum increases with decreasing bias current and at the same time the position of the maximum is shifted towards lower values of  $\omega$ . A decrease of the bias current causes (see next section on transient dynamics of a JJ) a decrease of the slope of the potential profile, which corresponds to a decreasing parameter  $k$  in our model (Eq. (8)). Therefore, the average lifetime maximum  $\tau_{-max}$  increases and as a consequence the time required to escape from the metastable fixed configuration  $\tau_{up}(D)$  increases too. Consequently, the corresponding rate of the barrier fluctuations  $\omega_{max} \simeq 1/\tau_{up}(D)$  decreases, as observed experimentally. Of course a more detailed analysis of the JJ system as a function of the temperature, that is the noise intensity, should add more interesting results.

Finally we note that in the frequency range  $\omega \in (10^{-5} \div 10^{-3})$ , for fixed values of the mean flipping rate, an overlap occurs in the curves for different values of the noise intensity. A nonmonotonic behavior of  $\tau_{-}(x_{in} = 0)$  as a function of the noise intensity is observed, as we expect in the transient dynamics of metastable states [3, 17, 23].

### 3. Transient dynamics in a Josephson junction

The investigation of thermal fluctuations and nonlinear properties of Josephson junctions (JJs) is very important owing to their broad applications in logic devices. Superconducting devices, in fact, are natural qubit candidates for quantum computing because they exhibit robust, macroscopic quantum behavior [31]. Recently, a lot of attention was devoted to Josephson logic devices with high damping because of their high-speed switching [18, 32]. The rapid single flux quantum logic (RSFQ), for example, is a superconductive digital technique in which the data are represented by the presence or absence of a flux quantum  $\Phi_0 = h/2e$ , in a cell which comprises Josephson junctions. The short voltage pulse corresponds to a single flux quantum moving across a Josephson junction, that is a  $2\pi$  phase

flip. This short pulse is the unit of information. However the operating temperatures of the high-Tc superconductors lead to higher noise levels by increasing the probability of thermally-induced switching errors. Moreover during the propagation within the Josephson transmission line fluxon accumulates a time jitter. These noise-induced errors are one of the main constraints to obtain higher clock frequencies in RSFQ microprocessors [32].

In this section, after a short introduction with the basic formulas of the Josephson devices, the model used to study the dynamics of a short overdamped Josephson junction is described. The interplay of the noise-induced phenomena RA and NES on the temporal characteristics of the Josephson devices is discussed. The role played by these noise-induced effects, in the accumulation of timing errors in RSFQ logic devices, is analyzed.

The Josephson tunneling junction is made up of two superconductors, separated from each other by a thin layer of oxide. Starting from Schrödinger equation and the two-state approximation model [33], it is straightforward to obtain the Josephson equation

$$\frac{d\varphi(t)}{dt} = \frac{2eV(t)}{\hbar}, \quad (20)$$

where  $\varphi$  is the phase difference between the wave function for the left and right superconductors,  $V(t)$  is the potential difference across the junction,  $e$  is the electron charge, and  $\hbar = h/2\pi$  is the Planck's constant. A small junction can be modelled by a resistance  $R$  in parallel with a capacitance  $C$ , across which is connected a bias generator and a phase-dependent current generator,  $I\sin\varphi$ , representing the Josephson supercurrent due to the Cooper pairs tunnelling through the junction. Since the junction operates at a temperature above absolute zero, there will be a white Gaussian noise current superimposed on the bias current. Therefore the dynamics of a short overdamped JJ, widely used in logic elements with high-speed switching and corresponding to a negligible capacitance  $C$ , is obtained from Eq. (20) and from the current continuity equation of the equivalent circuit of the Josephson junction. The resulting equation is the following Langevin equation

$$\omega_c^{-1} \frac{d\varphi(t)}{dt} = -\frac{du(\varphi)}{d\varphi} - i_F(t), \quad (21)$$

valid for  $\beta \ll 1$ , with  $\beta = 2eI_c R^2 C / \hbar$  the McCumber–Stewart parameter,  $I_c$  the critical current, and  $i_F(t) = \frac{I_F}{I_c}$ , with  $I_F$  the random component of the current. Here

$$u(\varphi, t) = 1 - \cos\varphi - i(t)\varphi, \quad \text{with } i(t) = i_0 + f(t), \quad (22)$$

is the dimensionless potential profile (see Fig. 4),  $\varphi$  is the difference in the phases of the order parameter on opposite sides of the junction,  $f(t) = A \sin(\omega t)$  is the driving signal,  $i = \frac{I}{I_c}$ ,  $\omega_c = \frac{2eR_N I_c}{\hbar}$  is the characteristic frequency of the JJ, and  $R_N$  is the normal state resistance (see Ref. [33]). When only thermal fluctuations are taken into account [33], the random current may be represented by the white Gaussian noise:  $\langle i_F(t) \rangle = 0$ ,  $\langle i_F(t) i_F(t + \tau) \rangle = \frac{2D}{\omega_c} \delta(\tau)$ , where  $D = \frac{2ekT}{\hbar I_c} = \frac{I_T}{I_c}$  is the dimensionless intensity of fluctuations,  $T$  is the temperature and  $k$  is the Boltzmann constant. The equation of motion Eq. (21) describes the overdamped motion

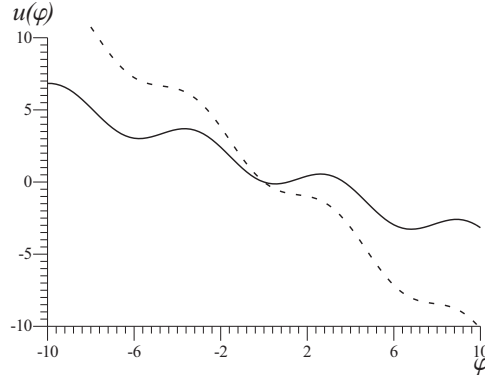


Fig. 4. The potential profile  $u(\varphi) = 1 - \cos\varphi - i\varphi$ , for values of the current, namely  $i = 0.5$  (solid line) and  $i = 1.2$  (dashed line).

of a Brownian particle moving in a washboard potential (see Fig. 4). A junction initially trapped in a zero-voltage state, with the particle localized in one of the potential wells, can escape out of the potential well by thermal fluctuations. The phase difference  $\varphi$  fluctuates around the equilibrium positions, minima of the potential  $u(\varphi)$ , and randomly performs jumps of  $2\pi$  across the potential barrier towards a neighbor potential minimum. The resulting time phase variation produces a nonzero voltage across the junction with marked spikes. For a bias current less than the critical current  $I_c$ , these metastable states correspond to "superconductive" states of the JJ. The mean time between two sequential jumps is the life time of the superconductive metastable state [25]. For an external current greater than  $I_c$ , the JJ junction switches from the superconductive state to the resistive one and the phase difference slides down in the potential profile, which now

has not equilibrium steady states. A Josephson voltage output will be generated in a later time. Such a time is the switching time, which is a random quantity. In the presence of thermal noise a Josephson voltage appears even if the current is less than the critical one ( $i < 1$ ), therefore we can identify the lifetime of the metastable states with the mean switching time [18, 25]. For the description of our system, i. e. a single overdamped JJ with noise, we will use the Fokker-Planck equation for the probability density  $W(\varphi, t)$ , which corresponds to the Langevin equation (21)

$$\frac{\partial W(\varphi, t)}{\partial t} = -\frac{\partial G(\varphi, t)}{\partial \varphi} = \omega_c \frac{\partial}{\partial \varphi} \left\{ \frac{du(\varphi)}{d\varphi} W(\varphi, t) + D \frac{\partial W(\varphi, t)}{\partial \varphi} \right\}. \quad (23)$$

The initial and boundary conditions of the probability density and of the probability current for the potential profile (22) are as follows:  $W(\varphi, 0) = \delta(\varphi - \varphi_0)$ ,  $W(+\infty, t) = 0$ ,  $G(-\infty, t) = 0$ . Let, initially, the JJ is biased by the current smaller than the critical one, that is  $i_0 < 1$ , and the junction is in the superconductive state. The current pulse  $f(t)$ , such that  $i(t) = i_0 + f(t) > 1$ , switches the junction into the resistive state. An output voltage pulse will appear after a random switching time. We will calculate the mean value and the standard deviation of this quantity for two different periodic driving signals: (i) a dichotomous signal, and (ii) a sinusoidal one. We will consider different values of the bias current  $i_o$  and of signal amplitude  $A$ . Depending on the values of  $i_o$  and  $A$ , as well as values of signal frequency and noise intensity, two noise-induced effects may be observed, namely the resonant activation (RA) and the noise enhanced stability (NES). Specifically the RA effect was theoretically predicted in Ref. [11] and experimentally observed in a tunnel diode [13] and in underdamped Josephson tunnel junctions [16, 20], and the NES effect was theoretically predicted in [22, 23, 25] and experimentally observed in a tunnel diode [3] and in an underdamped Josephson junction [20]. The RA and NES effects, however, have different role on the behavior of the temporal characteristics of the Josephson junction. They occur because of the presence of metastable states, in the periodic potential profile of the Josephson tunnel junction, and the thermal noise. Specifically, the RA phenomenon minimizes the switching time and therefore also the timing errors in RSFQ logic devices, while the NES phenomenon increases the mean switching time producing a negative effect [18].

### 3.1. Temporal characteristics

Now we investigate the following temporal characteristics: the mean switching time (MST) and its standard deviation (SD) of the Josephson

junction described by Eq. (21). These quantities may be introduced as characteristic scales of the evolution of the probability  $P(t) = \int_{\varphi_1}^{\varphi_2} W(\varphi, t) d\varphi$ , to find the phase within one period of the potential profile of Eq. (22). We choose therefore  $\varphi_2 = \pi$ ,  $\varphi_1 = -\pi$  and we put the initial distribution on the bottom of a potential well:  $\varphi_0 = \arcsin(i_0)$ . A widely used definition of such characteristic time scales is the integral relaxation time (see the paper by Malakhov and Pankratov in Ref [12]). Let us summarize shortly the results obtained in the case of dichotomous driving,  $f(t) = A \text{sign}(\sin(\omega t))$ . Both MST and its SD do not depend on the driving frequency below a certain cut-off frequency (approximately  $0.2\omega_c$ ), above which the characteristics degrade. In the frequency range from 0 to  $0.2\omega_c$ , therefore, we can describe the effect of dichotomous driving by time characteristics in a constant potential. The exact analytical expression of the first two moments of the switching time are [18]

$$\tau_c(\varphi_0) = \frac{1}{D\omega_c} \left[ \int_{\varphi_0}^{\varphi_2} e^{\frac{u(x)}{D}} \int_{\varphi_1}^x e^{-\frac{u(\varphi)}{D}} d\varphi dx + \int_{\varphi_1}^{\varphi_2} e^{-\frac{u(\varphi)}{D}} d\varphi \int_{\varphi_2}^{\infty} e^{\frac{u(\varphi)}{D}} d\varphi \right], \quad (24)$$

and

$$\tau_{2c}(\varphi_0) = \tau_c^2(\varphi_0) - \int_{\varphi_0}^{\varphi_2} e^{-\frac{u(x)}{D}} H(x) dx - H(\varphi_0) \int_{\varphi_1}^{\varphi_0} e^{-\frac{u(x)}{D}} dx, \quad (25)$$

where  $H(x) = \frac{2}{(D\omega_c)^2} \int_x^{\infty} e^{u(v)/D} \int_v^{\varphi_2} e^{-u(y)/D} \int_y^{\infty} e^{u(z)/D} dz dy dv$ . The asymptotic expressions of the MST and its standard deviation (SD), obtained in the small noise limit ( $D \ll 1$ ), agree very well with computer simulations up to  $D = 0.05$  [18]. Therefore, not only low temperature devices ( $D \leq 0.001$ ), but also high temperature devices may be described by these expressions. If the noise intensity is rather large, the phenomenon of NES may be observed in our system: the MST increases with the noise intensity. Here we note that it is very important to consider this effect in the design of large arrays of RSFQ elements, operating at high frequencies. To neglect this noise-induced effect in such nonlinear devices it may lead to malfunctions due to the accumulation of errors.

Now let us consider the case of sinusoidal driving. The corresponding time characteristics may be derived using the modified adiabatic approximation [14, 18]

$$P(\varphi_0, t) = \exp \left\{ - \int_0^t \frac{1}{\tau_c(\varphi_0, t')} dt' \right\}, \quad (26)$$

with  $\tau_c(\varphi_0, t')$  given by Eq. (24), after inserting in this equation the time dependent potential profile  $u(\varphi, t)$  of Eq. (22). Using the relation  $\tau = \int_0^{+\infty} P(\varphi_0, t) dt$  we calculate the MST. We focus now on the current value  $i = 1.5$ , because  $i = 1.2$  is too small for high frequency applications. In Fig. 5 the MST and its SD as a function of the driving frequency, for three values of the noise intensity ( $D = 0.02, 0.05, 0.5$ ), for a bias current  $i_0 = 0.5$ , and  $A = 1$  are shown. We note that, because  $\varphi_0 = \arcsin(i_0)$  depends on  $i_0$ , the switching time is larger for smaller  $i_0$ . However, great bias current values  $i_0$ , in the absence of driving, give rise to the reduction of the mean life time of superconductive state, i.e. to increasing storage errors (Eq. (24)). Therefore, there must be an optimal value of bias current  $i_0$ , giving minimal switching time and acceptably small storage errors. We observe the phenomenon of resonant activation: MST has a minimum as a function of driving frequency.

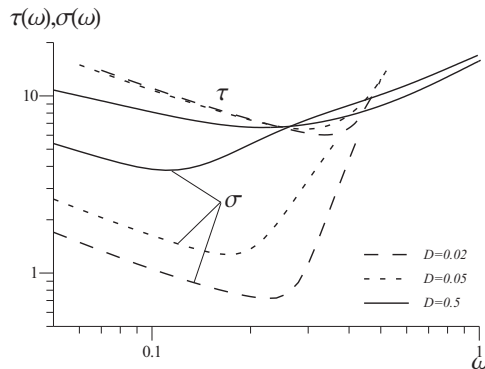


Fig. 5. The MST and its SD vs frequency for  $f(t) = A \sin(\omega t)$  (computer simulations) for three values of the noise intensity. Namely: Long-dashed line -  $D = 0.02$ , short-dashed line -  $D = 0.05$ , solid line -  $D = 0.5$ . The value of the bias current is  $i_0 = 0.5$ , and the total current is  $i = 1.5$ .

The approximation (26) works rather well below  $0.1 \omega_c$ , that is enough for practical applications (see the inset of Fig. 3 in ref. [18]). It is interesting to see that near the minimum the MST has a very weak dependence on the noise intensity (as it is clearly shown in the  $\tau$  behavior of Fig. 5 for three values of the noise intensity), i. e. in this signal frequency range the noise is effectively suppressed. This noise suppression is due to the resonant activation phenomenon: a minimum appears in the MST and SD, when the escape process is strongly correlated with the potential profile oscillations. A noise suppression effect, but due to the noise, is reported in Ref. [34]. We observe also the NES phenomenon. There is a frequency range in Fig. 5, around  $(0.2 \div 0.48)\omega_c$  for  $i_0 = 0.5$ , where the switching

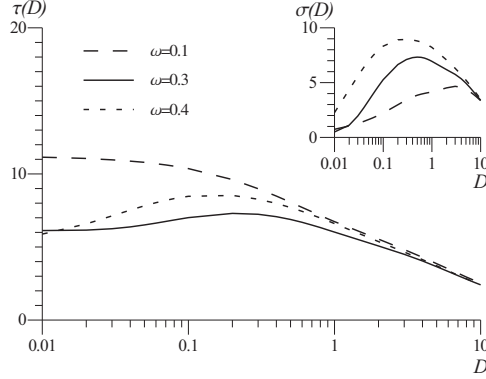


Fig. 6. The MST vs noise intensity for  $f(t) = A \sin(\omega t)$  and for three values of the driving frequency. Namely:  $\omega = 0.1$  (long-dashed line),  $\omega = 0.3$  (short-dashed line),  $\omega = 0.4$  (solid line). Inset: The standard deviation (SD) vs noise intensity for the same values of driving frequency  $\omega$ .

time increases with the noise intensity. To see in more detail this effect we report in Fig. 6 the MST  $\tau(D)$  and its SD  $\sigma(D)$  vs the noise intensity  $D$ , for three fixed values of the driving frequency, namely:  $\omega = 0.1, 0.3, 0.4$ . Both quantities have nonmonotonic behaviour and the great values of  $\sigma(D)$  near the maximum of  $\tau(D)$  confirm that the only information on the MST is not sufficient to fully unravel the statistical properties of the NES effect [24]. A detailed analysis of the PDF of the lifetime during the transient dynamics is required. This is subject of a forthcoming paper. Simulations for different bias current values [18] show that the NES effect increases for smaller  $i_0$  because the potential barrier disappears for a short time interval within the driving period  $T = 2\pi/\omega$  and the potential is more flat [3]. The noise, therefore, has more chances to prevent the phase to move down and the switching process is delayed. This effect may be avoided, if the operating frequency does not exceed  $0.2 \omega_c$ . Besides the SD and MST (see Fig. 5) have their minima in a short range of values of  $\omega$  [18]. Close location of minima of MST and its SD means that optimization of RSFQ circuit for fast operation will simultaneously lead to minimization of timing errors in the circuit.

#### 4. Dynamics of a FHN stochastic model

##### 4.1. Suppression of noise and noise-enhanced stability effect

*Case I.* Let us fix the value of the noise intensity and analyze The analysis of the stochastic properties of neural systems is of particular importance since it plays an important role in signal transmission [19], [35]-[41]. Bio-

logically realistic models of the nerve cells, such as widely-known Hodgkin-Huxley (HH) system [35], are so complex that they provide little intuitive insight into the neuron dynamics that they simulate. The FitzHugh-Nagumo (FHN) model, however, which is one of the simplified modifications of HH, is more preferable for investigation [41]. Nevertheless many effects observed in neural cells are qualitatively contained in FHN model. Because of this the FHN model has got wide dissemination in the last few years. There has been a lot of papers where the influence of noise on the encoding sensitivity of a neuron in the framework of FHN model has been analyzed. A broad spectrum of noise-induced dynamical effects, which produce ordered periodicity in the output of the FHN system, has been discovered. Among these effects we cite the coherence resonance [36] and the stochastic resonance (SR) [37]. All these investigations deal with neuron dynamics with subthreshold signals, and with an enhancement of a weak signal through the noise. The presence of noise in the case of a strong periodic forcing, however, has a detrimental effect on the encoding process [38]-[40]. For suprathreshold signals the noise always lowers the information transmission, and the SR effects disappear [38, 39]. However, as it was shown in recent papers of Stocks [40], this is only true for a single element threshold system. In neuronal arrays the noise can significantly enhance the information transmission when the signal is predominantly suprathreshold. It is the effect of suprathreshold stochastic resonance.

Here we analyze the effect of noise in a single neuron subjected to a strong periodic forcing. We investigate therefore, the influence of noise on the appearance time of a first spike, or the mean response time, in the output of FHN model with periodical driving in suprathreshold regime. As it was mentioned before, the role of noise for a strong driving is negative. In this case noise suppresses the response of a neuron, that leads to delay of transmission of an external information. But we show that, this negative influence of noise on the spike generation can be significantly minimized.

We analyze the dependencies of the mean response time (MRT) on both driving frequency and noise intensity. We find that, MRT plotted as a function of the driving frequency shows a resonant activation-like phenomenon. The noise enhanced stability (NES) effect is also observed here. It is shown that MRT can be increased due to the effect of fluctuations. We note that NES has nothing to do with the typical SR, where the maximum of signal to noise ratio as a function of noise intensity is observed. There are many differences between these effects concerning the neuron dynamics. First of all the SR is related to the output of the neuron in stationary dynamical regime and concerns the signal-to-noise ratio, while the NES describes the transient dynamical regime of a neuron and concerns the mean response time. In addition there is difference in the nature of the response: We



investigate the case of a strong driving, where the SR effects disappear.

#### 4.2. Deterministic dynamical regime

The dynamic equations of the FitzHugh-Nagumo model with additive periodic forcing are

$$\begin{aligned}\dot{x} &= x - x^3/3 - y + A \sin(\omega t) \\ \dot{y} &= \epsilon(x + I),\end{aligned}\tag{27}$$

where  $x$  is the voltage,  $y$  is the recovery variable, and  $\epsilon$  is a fixed small parameter ( $\epsilon = 0.05$ ). In the absence of both external driving and noise, there is only one steady state of the system (27), that is  $x_0 = -I$ ;  $y_0 = -I + I^3/3$ . The choice of the constant  $I$ , therefore, fully specifies the location of equilibrium state in the phase space  $(x, y)$ . Here we consider  $I = 1.1$ .

In our simulations we assume that the initial conditions for each realization are the same, that is the system is in its stable equilibrium point (the rest state)  $(x_0, y_0)$  at the initial time  $t_0$ . We would like to note, here, that even if we consider sinusoidal driving, we investigate the time of appearance of the first spike only. We are interested in the capability of our system to detect an external input. This means to minimize the detection time and to get a neuron response that would be more robust to the noise action. After generation of the first spike, that is after approaching of the boundary  $x = 0$ , we break the realization off, and start a new one with the same initial conditions  $(x_0, y_0)$ .

For our system the threshold value of the driving amplitude required for spike generation is  $A_{th} \sim 0.05$ . In our simulations we choose  $A = 0.5$ . Thus, the frequency range where the signal of such amplitude is suprathreshold is:  $\Omega : \omega \in (0.013 \div 1.9)$  [19]. Inside this region  $\Omega$  the response time of a neuron has a minimum as a function of the driving frequency. System does not respond outside the range  $\Omega$ . Here, a subthreshold oscillation occurs (see Fig. 7(b)). In Fig. 7(c) the time series of the output voltage  $x$  for a suprathreshold signal is shown.

#### 4.3. Suprathreshold stochastic regime

Actually, there are many factors that make the environment noisy in the neuron dynamics. Among them we cite the fluctuating opening and closure of the ion channels within the cell membrane, the noisy presynaptic currents, and others (see, for example, Ref. [36]). We consider two different cases in which the noise is added to the first or the second equation of the system (27):

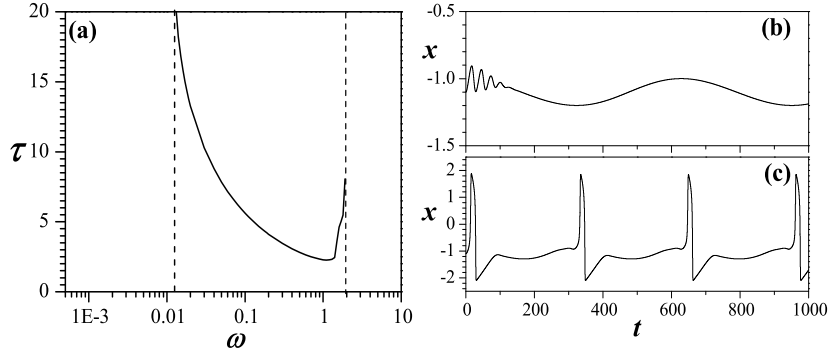


Fig. 7. (a) The response time dependence versus the frequency of periodic driving for the deterministic case,  $A = 0.5$ . Examples of output trajectory for two values of driving frequency invoking two different kinds of oscillations: (b) subthreshold for  $\omega = 0.01$ , and (c) suprathreshold for  $\omega = 0.02$ .

Case I The variable that corresponds to the membrane potential is subjected to fluctuations [37, 40]. In this case, the first equation of the system (27) becomes the following stochastic differential equation

$$\dot{x} = x - x^3/3 + A \sin(\omega t) - y + \xi(t); \quad (28)$$

Case II The recovery variable associated with the refractory properties of a neuron is noisy [36]. Here, the second equation of the system (27) becomes

$$\dot{y} = \epsilon(x + I) + \xi(t), \quad (29)$$

In Eqs. (28) and (29),  $\xi(t)$  is a Gaussian white noise with zero mean and correlation function  $\langle \xi(t)\xi(t+\tau) \rangle = D\delta(\tau)$ . For numerical simulations we use the modified midpoint method and the noise generator routine reported in Ref [42].

The mean response time (MRT) of our neuronal system is obtained as the mean first passage time at the boundary  $x = 0$ :  $\tau = \langle T \rangle = \frac{1}{N} \sum_{i=1}^N T_i$ , where  $T_i$  is the response time for  $i$ -th realization. To obtain smooth average for all the noise values investigated, we need different number of realizations  $N$  in above considered cases. Namely,  $N = 5000$  in case *I*, and  $N = 15000$  in case *II*, specifically when the noise intensities are comparable with the value of the parameter  $\epsilon = 0.05$ . It is worth noting here that parameter  $T_i$  characterizes the delay of the systems' response, and has a non-zero value even in the deterministic case, because of the non-instantaneous neuronal

response. In our investigation we consider a strong driving, so the noise increases the time of appearance of the first spike and leads to an additional delay of the signal detection.

the MRT dependence on the driving frequency. In the small noise limit  $D \rightarrow 0$ , a typical behavior (see Fig. 8) with perpendicular walls disposed at the frequencies corresponding to the boundaries of the region  $\Omega$  was found. By increasing the noise intensity, these walls go down. We observe a resonant activation-like phenomenon: The MRT exhibits a minimum as a function of the driving frequency, which is almost independent of the noise intensity.

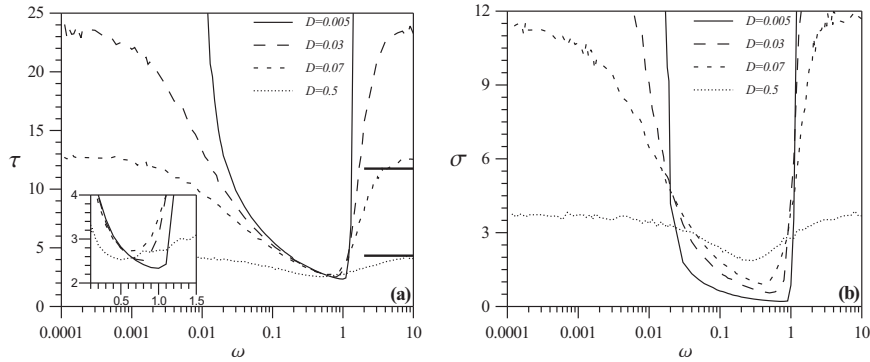


Fig. 8. (a) The mean response time dependence versus the frequency of periodic driving for case  $I$ , for four values of the noise intensity, namely:  $D = 0.005, 0.03, 0.07, 0.5$ . The right solid lines give the theoretical values of  $\tau$  for fixed bistable potential. Inset: frequency range where the noise enhanced stability effect is observed. (b) The standard deviation of the response time dependence vs frequency of periodic driving for case  $I$ , for the same values of  $D$ .

In the same figure (b) the standard deviation (SD) of the response time versus the frequency of the periodic driving shows a minimum. Therefore, the noise has minimal effect in the same range of driving frequencies for MRT and its SD. In a narrow frequency range ( $\omega \in (0.6 \div 1.3)$ ) (see Fig. 8), we found a nonmonotonic behavior of the MRT as a function of the noise intensity. Here the noise enhanced stability effect is observed (see the inset of Fig. 8a). Out of this range the MRT monotonically decreases with increasing noise intensity. For larger noise intensities the MRT dependence on driving frequency takes a constant-like behavior in the range of the investigated frequency values ( $\omega \in [10^{-4} \div 10]$ ). Here, the dynamics of the system is mainly controlled by the noise, and the frequency of periodic driving does not affect significantly the neuron response dynamics. By numerical simulations of our system we find that, for large noise intensities, the MRT

coincides with that calculated by standard technique for a Brownian particle moving in a bistable fixed potential [44]

$$\tau = 2/D \int_{x_0}^0 e^{\varphi(x)/D} \int_{\infty}^x e^{-\varphi(y)/D} dy dx. \quad (30)$$

The theoretical values reported in Fig. 8(a) agree with the limiting values of  $T$  for  $\omega \rightarrow 0$  and  $\omega \rightarrow \infty$ . For  $\epsilon \ll 1$  in fact,  $x$  is a fast variable and  $y$  is a slow variable, so  $\dot{y} \simeq 0$  and this case can be recast as an escape problem from a one-dimensional double well in both limiting cases. In fact when  $\omega \rightarrow 0$  we have a fixed bistable potential, and for  $\omega \rightarrow \infty$  we have an average fluctuating potential, which coincides with the fixed one. This is well visible in Fig. 8(a) for  $D = 0.07$ . For  $D = 0.5$  the MRT tends to be almost independent on the parameter  $\omega$ .

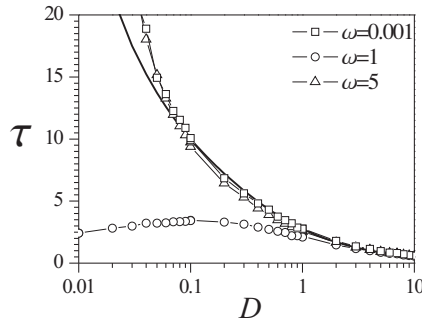


Fig. 9. The mean response time dependence versus the noise intensity for case  $I$ , for three different values of driving frequency:  $\omega = 0.001$ ,  $\omega = 1$  and  $\omega = 5$ . Solid line gives the theoretical values of  $\tau$  for fixed bistable potential.

In Fig. 9 the MRT versus the noise intensity, for three values of the driving frequency, is shown. We see the nonmonotonic behavior for  $\omega = 1$ , which is a signature of the NES effect. It is interesting to note that even in this system, whose global dynamics cannot be described as the motion of a Brownian particle in a potential profile (because of the coupling between the two stochastic differential equations describing our system) a phase transition-like phenomenon, with respect to the driving frequency parameter  $\omega$ , occurs. In fact we have nonmonotonic and monotonic behavior depending on the value of  $\omega$ . We expect similar behavior, if we fix the driving frequency and we change the value of the amplitude  $A$  of the driving force [3, 17].

*Case II.* In this case, for noise intensity values greater than  $\epsilon = 0.05$ , the recover variable can be approximated by a Wiener process ( $\dot{y} \approx \xi(t)$ ). This process acts now as a noise source in the same double well potential according the following stochastic differential equation

$$\dot{x} = x - x^3/3 + A \sin(\omega t) + W(t), \quad (31)$$

where  $W(t)$  is the Wiener process with the usual statistical properties:  $\langle W(t) \rangle = 0$ , and  $\langle W^2(t) \rangle = t$ .

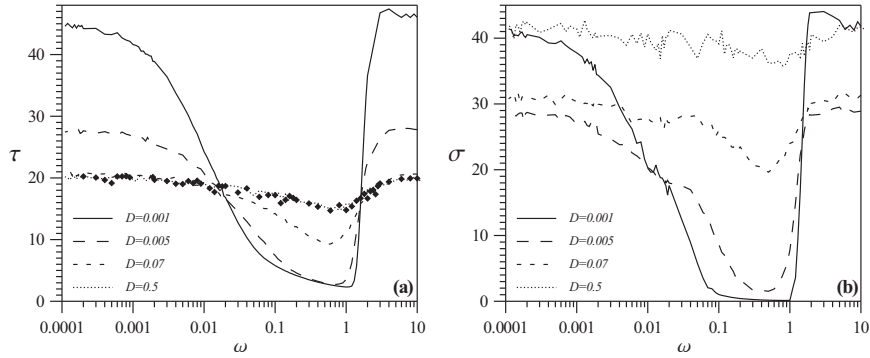


Fig. 10. (a) The mean response time dependence vs the frequency of the periodic driving for case *II*, for four values of the noise intensity, namely:  $D = 0.001, 0.005, 0.07, 0.5$ . The curve with diamonds gives the values of  $\tau$  for fixed bistable potential, when the noise source is a Wiener process. (b) The standard deviation of the response time dependence vs frequency of periodic driving for case *II*.

In Fig. 10(a) the curve with diamonds shows the results of this approximation for  $D = 0.5$ . We found again a resonant activation-like phenomenon (see Fig. 10), which is independent of the noise intensity, as in case *I*, until  $D$  reaches the value of parameter  $\epsilon$ . The minimum tends to disappear for greater noise intensities. Here a certain frequency range ( $\omega \in (0.019 \div 1.6)$ ), larger than in previous case, exists where an increasing noise intensity leads to a monotonic growth of the MRT. Out of this range the MRT monotonically decreases with increasing noise intensity, as in case *I*. In Fig. 10(b) the standard deviation of the response time versus the driving frequency is shown. Also in this case *II*, the SD shows a minimum in the same frequency range of that found for MRT. We have found, therefore, a parameter region where there is minimization of the MRT and its SD, that is "suppression of noise".

We also observe that the saturation level reached in each case is different. Particularly in case *II* it is greater than in case *I*, because the MRT is calculated with respect to the membrane voltage  $x$  and with different noise

sources. Therefore, in phase space the variable  $x$  reaches, in case *I*, in a minor average time the boundary  $x = 0$ , according to Eq. (28). While in case *II* the variation of  $x$  depends on the dynamics of the  $y$  coordinate and takes much more time to reach the same boundary.

### 5. A stochastic model for cancer growth dynamics

In this last section we shortly summarize some of the main results obtained with a stochastic model for cancer growth dynamics (see Ref. [21] for more details). Most of tumoral cells bear antigens which are recognized as strange by the immune system. A response against these antigens may be mediated either by immune cells such as T-lymphocytes or other cells like macrophages. The process of damage to tumor proceeds via infiltration of the latter by the specialized cells, which subsequently develop a cytotoxic activity against the cancer cell-population. The series of cytotoxic reactions between the cytotoxic cells and the tumor tissue have been documented to be well approximated by a saturating, enzymatic-like process whose time evolution equations are similar to the standard Michaelis-Menten kinetics [45, 46]. The T-helper lymphocytes and macrophages, can secrete cytokines in response to stimuli. The functions that cytokines induce can both "turn on" and "turn off" particular immune responses [47, 48]. This "on-off" modulating regulatory role of the cytokines is here modelled through a dichotomous random variation of the parameter  $\beta$ , which is responsible for regulatory inhibition of the population growth, by taking into account the natural random fluctuations always present in biological complex systems.

The dynamical equation of this biological system is

$$\dot{x} = -\frac{dU^\pm(x)}{dx} + \xi(t), \quad (32)$$

where  $\xi(t)$  is a Gaussian process with  $\langle \xi(t) \rangle = 0$ ,  $\langle \xi(t)\xi(t') \rangle = D\delta(t - t')$ , and

$$U^\pm(x) = -\frac{x^2}{2} + \frac{\theta x^3}{3} + (\beta_o \pm \Delta)(x - \ln(x + 1)), \quad (33)$$

is the stochastic double well Michaelis-Menten potential with one the minima at  $x = 0$ . Here  $x(t)$  is the concentration of the cancer cells. The process  $\beta = (\beta_o \pm \Delta)$  can change the relative stability of the metastable state of the potential profile [46]. We note that the RA and NES phenomena act counter to each other in the cancer growth dynamics: the NES effect increases in an unavoidable way the average lifetime of the metastable state (associated to a fixed-size tumor state), while the RA phenomenon minimizes this lifetime. Therefore it is crucial to find the optimal range of parameters in which the

positive role of resonant activation phenomenon, with respect to the cancer extinction, prevails over the negative role of NES, which enhances the stability of the tumoral state. These are just the main results of the paper [21], that is both NES and RA phenomena are revealed in a biological system with a metastable state, with a co-occurrence region of these effects. In this coexistence region the NES effect, which enhances the stability of the tumoral state, becomes strongly reduced by the RA mechanism, which enhances the cancer extinction. In other words, an asymptotic regression to the zero tumor size may be induced by controlling the modulating stochastic activity of the cytokines on the immune system.

## 6. Conclusions

Natural systems are open to the environment. Consequently, in general, stationary states are not equilibrium states, but are strongly influenced by dynamics, which adds further challenge to the microscopic understanding of metastability. The investigation of two noise-induced effects in far from equilibrium systems, namely the RA and NES phenomena, has revealed interesting peculiarities of the dynamics of these systems. Specifically the knowledge of the parameter regions where the RA and NES can be revealed allows:

- to optimize and to suppress timing errors in practical RSFQ devices, and therefore to significantly increase working frequencies of RSFQ circuits;
- to optimize the operating range of a neuron, and therefore to realize high rate signal transmission with the suppression of noise;
- to maximize or minimize the extinction time in cancer growth population dynamics.

## 7. Acknowledgments

This work was supported by MIUR, INFN-CNR and CNISM, Russian Foundation for Basic Research (Projects No. 05-01-00509 and No. 05-02-19815), and ESF (European Science Foundation) STOCHDYN network. E.V.P. also acknowledges the support of the Dynasty Foundation.

## REFERENCES

- [1] J.D. Gunton, M. Droz, *Introduction to the Theory of Metastable and Unstable States*, Springer, Berlin, 1983.

- [2] A. J. Leggett, *Phys. Rev. Lett.* **53**, 1096 (1984); M. Muthukumar, *ibid.* **86**, 3188 (2001).
- [3] R. N. Mantegna and B. Spagnolo, *Phys. Rev. Lett.* **76**, 563 (1996); *Int. J. Bifurcation and Chaos* **4**, 783 (1998).
- [4] A. Strumia, N. Tetradis, *JHEP* **11**, 023 (1999).
- [5] P.G. Debenedetti, F.H. Stillinger, *Nature* **410**, 267 (2001).
- [6] R. H. Victora, *Phys. Rev. Lett.* **63**, 457 (1989).
- [7] Y.W. Bai et al, *Science* **269**, 192 (1995).
- [8] O. A. Tretiakov, T. Gramespacher, and K. A. Matveev, *Phys. Rev. B* **67**, 073303 (2003).
- [9] M. Gleiser, R.C. Howell, *Phys. Rev. Lett.* **94**, 151601 (2005).
- [10] G. Parisi, *Nature* **433**, 221 (2005); S. Kraut and C. Grebogi, *Phys. Rev. Lett.* **93**, 250603 (2004); H. Larralde and F. Leyvraz, *ibid.* **94**, 160201 (2005); G. Báez et al., *ibid.* **90**, 135701 (2003).
- [11] C. R. Doering and J. C. Gadoua, *Phys. Rev. Lett.* **69**, 2318 (1992).
- [12] M. Bier and R. D. Astumian, *Phys. Rev. Lett.* **71**, 1649 (1993); P. Pechukas and P. Hänggi, *ibidem* **73**, 2772 (1994); J. Iwaniszewski, *Phys. Rev. E* **54**, 3173 (1996); M. Boguñá, J. M. Porra, J. Masoliver, and K. Lindenberg, *ibidem* **57**, 3990 (1998); M. Bier, I. Derenyi, M. Kostur, D. Astumian, *ibidem* **59**, 6422 (1999); A. L. Pankratov and M. Salerno, *Phys. Lett. A* **273**, 162 (2000); A. N. Malakhov and A. L. Pankratov, *Adv. Chem. Phys.* **121**, 357 (2002).
- [13] R. N. Mantegna and B. Spagnolo, *Phys. Rev. Lett.* **84**, 3025 (2000); *J. Phys. IV (France)* **8**, 247 (1998).
- [14] A. L. Pankratov and M. Salerno, *Phys. Lett. A* **273**, 162 (2000).
- [15] B. Dybiec, E. Gudowska-Nowak, *Phys. Rev. E* **66**, 026123 (2002).
- [16] Y. Yu and S. Han, *Phys. Rev. Lett.* **91**, 127003 (2003).
- [17] A. A. Dubkov, N. V. Agudov and B. Spagnolo, *Phys. Rev. E* **69**, 061103 (2004).
- [18] A. L. Pankratov and B. Spagnolo, *Phys. Rev. Lett.* **93**, 177001 (2004).
- [19] E. V. Pankratova, A. V. Polovinkin, and B. Spagnolo, *Physics Letters A* **344**, 43-50 (2005).
- [20] G. Sun et al., *Phys. Rev. E* **75**, 021107(4) (2007).
- [21] A. Fiasconaro and B. Spagnolo, A. Ochab-Marcinek and E. Gudowska-Nowak, *Phys. Rev. E* **74**, 041904(10) (2006); A. Ochab-Marcinek, E. Gudowska-Nowak, A. Fiasconaro and B. Spagnolo, *Acta Physica Polonica B* **37** (5), 1651 (2006).
- [22] J. E. Hirsch, B. A. Huberman, and D. J. Scalapino, *Phys. Rev. A* **25**, 519 (1982); I. Dayan, M. Gitterman, and G. H. Weiss, *ibidem* **46**, 757 (1992); R. Wackerbauer, *Phys. Rev. E* **59**, 2872 (1999); D. Dan, M. C. Mahato, and A. M. Jayannavar, *ibidem* **60**, 6421 (1999); A. Mielke, *Phys. Rev. Lett.* **84**, 818 (2000); C. Xie and D. Mei, *Chin. Phys. Lett.* **20**, 813 (2003).
- [23] N. V. Agudov and B. Spagnolo, *Phys. Rev. E* **64**, 035102(R) (2001).



- [24] A. Fiasconaro, B. Spagnolo and S. Boccaletti, *Phys. Rev. E* **72**, 061110(5) (2005); A. Fiasconaro, D. Valenti, B. Spagnolo, *Physica A* **325**, 136-143 (2003).
- [25] A. N. Malakhov and A.L. Pankratov, *Physica C* **269**, 46 (1996).
- [26] N. V. Agudov and A. N. Malakhov, *Phys. Rev. E* **60**, 6333 (1999).
- [27] B. Spagnolo, A. A. Dubkov, and N. V. Agudov, *Eur. Phys. J. B* **40**, 273-281 (2004); B. Spagnolo, A. A. Dubkov, N. V. Agudov, *Acta Physica Polonica B* **35**, 1419 (2004).
- [28] H. A. Kramers, *Physica* **7**, 284 (1940).
- [29] P. Hänggi, P. Talkner, and M. Borkovec, *Rev. Mod. Phys.* **62**, 251 (1990).
- [30] A. N. Malakhov, *Chaos* **7**, 488 (1997).
- [31] Y. Makhlin, G. Schön, and A. Shnirman, *Rev. Mod. Phys.* **73**, 357 (2001); Y. Yu *et al.*, *Science* **296**, 889 (2002).
- [32] T. Ortlev, H. Toepfer and H. F. Uhlmann, *IEEE Trans. Appl. Supercond.* **13**, 515 (2003); V. Kapluneko, *Physica C* **372-376**, 119 (2002).
- [33] A. Barone and G. Paterno, *Physics and Applications of the Josephson Effect*, Wiley, 1982.
- [34] J. M. G. Vilar and J. M. Rubí, *Phys. Rev. Lett.* **86**, 950 (2001).
- [35] S. Lee, A. Neiman, and S. Kim, *Phys. Rev. E* **57**, 3292 (1998).
- [36] A.S. Pikovsky and J. Kurths, *Phys. Rev. Lett.* **78**, 775 (1997); B. Lindner and L. Schimansky-Geier, *Phys. Rev. E* **60**, 7270 (1999).
- [37] A. Longtin, D. Chialvo, *Phys. Rev. Lett.* **81**, 4012 (1998); L. Gammaitoni, P. Hänggi, P. Jung, and F. Marchesoni, *Rev. Mod. Phys.* **70**, 254 (1998).
- [38] A.R. Bulsara and A. Zador, *Phys. Rev. E* **54**, R2185 (1996).
- [39] J.E. Levin and J.P. Miller, *Nature* **380**, 165 (1996).
- [40] N.G. Stocks and R. Mannella, *Phys. Rev. E* **64**, 030902 (2001); N.G. Stocks, D. Allingham, and R.P. Morse, *Fluctuation and Noise Lett.* **2**, L169 (2002).
- [41] R. Fitzhugh, *Biophys. J.* **1**, 445-466 (1961); J.S. Nagumo, S. Arimoto, and S. Yoshizawa, *Proc. Inst. Radio Engineers* **50**, 2061-2070 (1962).
- [42] W. Press, B. Flannery, S. Teukolsky, and W. Vetterling *Numerical Recipes in C*, Cambridge University Press, Cambridge, 1993.
- [43] L.A. Pontryagin, A.A. Andronov, and A.A. Vitt, *Zh. Eksp. Teor. Fiz.* **3**, 165 (1933).
- [44] C. W. Gardiner, *Handbook of Stochastic Methods*, (Springer, Berlin, 2004).
- [45] R.P. Garay and R. Lefever, *J. Theor. Biol.* **73**, 417 (1978); R. Lefever, W. Horsthemke, *Bull. of Math. Biol.* **41**, 469 (1979).
- [46] A. Ochab-Marcinek and E. Gudowska-Nowak, *Physica A* **343**, 557 (2004).
- [47] A. Mantovani, A. Sica, *et al.*, *Trends Immunol.* **25**, 677 (2004); A. Mantovani, P. Allavena, A. Sica, *Eur. J. Cancer* **40**, 1660 (2004).
- [48] R. L. Elliott and G. C. Blobe, *J. Clin. Oncol.* **23**, 2078 (2005).